HHS Public Access

Author manuscript

Nat Med. Author manuscript; available in PMC 2011 August 01.

Published in final edited form as:

Nat Med. 2011 February ; 17(2): 206–210. doi:10.1038/nm.2295.

Hyperglycemia Induced Cerebral Hematoma Expansion is Mediated by Plasma Kallikrein

Jia Liu[1,4], **Ben-Bo Gao**[1,4], **Allen C. Clermont**[1], **Price Blair**[2], **Tamie J. Chilcote**[3], **Sukanto Sinha**[3], **Robert Flaumenhaft**[2], and **Edward P. Feener**[1]

[1]Research Division, Joslin Diabetes Center, One Joslin Place, Boston, Massachusetts 02215, USA. Department of Medicine, Harvard Medical School, 25 Shattuck Street Boston, Massachusetts, 02115, USA.

[2]Department of Medicine, Division of Hemostasis and Thrombosis, Beth Israel Deaconess Medical Center, Harvard Medical School, Boston, MA 02215, USA.

[3]ActiveSite Pharmaceuticals Inc., 1456 Fourth St., Unit C, Berkeley CA 94710.

Abstract

Hyperglycemia is associated with increased hematoma expansion and worse clinical outcomes following intracerebral hemorrhage. We demonstrate that cerebral hematoma expansion triggered by intracerebral infusion of autologous blood is increased in diabetic rats and mice, and this response is ameliorated by plasma kallikrein (PK) inhibition and deficiency, respectively. Both diabetes and hyperglycemia induced in nondiabetic rats increase hematoma expansion following intracerebral injection of purified PK, a response not observed with bradykinin, plasmin, or tissue plasminogen activator. This response is rapid, prevented by co-injection of the glycoprotein VI (GPVI) agonist convulxin, and mimicked by GPVI inhibition or deficiency. We show that PK binding to collagen and PK-mediated inhibition of collagen-induced platelet aggregation is enhanced by hyperglycemia. Hyperosmotic mannitol also increases hematoma expansion induced by blood and PK, and increases PK-mediated inhibition of platelet aggregation. These findings suggest that hyperglycemia increases cerebral hematoma expansion by PK-mediated osmotic-sensitive inhibition of hemostasis.

Intracerebral hemorrhage (ICH) accounts for 7–20% of all cases of stroke and overall case-fatality within 1 month is 42%1. Both diabetes and admission hyperglycemia are independently associated with early and long-term mortality after ICH2–5. In addition,

Corresponding author: Edward P Feener, PhD, Joslin Diabetes Center, 1 Joslin Place, Boston MA, 02215, Fax number: 617-309-2637, Telephone number: 617-309-2599, Edward.Feener@joslin.harvard.edu.

[4]These authors contributed equally to this work.

AUTHOR CONTRIBUTIONS

J.L. initiated, designed, and conducted most of the experiments and wrote the manuscript. B.-B.G. contributed to the design and performance of animal studies, biochemical analyses, platelet studies, and manuscript writing. A.C.C. contributed to animal studies. P.B. and R.H. designed and performed studies using platelet aggregometer and contributed to data interpretation. T.J.C. and S.S. contributed to data interpretation and manuscript editing. E.P.F. designed and supervised the entire study and contributed to manuscript writing.

hyperglycemia is independently associated with symptomatic ICH in stroke patients treated with intravenous tissue plasminogen activator (tPA)6–7. Hematoma volume is a significant, independent determinant of worse clinical outcomes after ICH8–9. While hyperglycemia is associated with increased hematoma volume and expansion3,10–14, little is known regarding the effects of hyperglycemia on hematoma expansion and cerebral hemostasis following vascular injury. Moreover, although over 50% of patients with stroke have hyperglycemia15, the clinical benefit of glucose normalization in the acute stroke setting is controversial16–17. Data on the clinical benefit of glucose lowering in ICH are limited and the potential therapeutic window for glucose lowering is unknown4,18–19. Recent guidelines suggest a judicious approach to the management of hyperglycemia in people with spontaneous ICH until additional clinical information is available20. In this report we investigated the effect of diabetes and hyperglycemia on acute hematoma expansion and the mechanisms that may contribute to hematoma expansion after experimental ICH.

We compared the response to intracerebral infusion of autologous whole blood in rats with 4-weeks of streptozotocin (STZ)-induced diabetes (DM) with age-matched nondiabetic (NDM) rats. This method was used to quantify the effect of diabetes on hemorrhagic response to a specific volume and location of intra-parenchymal blood, thereby assessing hematoma expansion independent of variables associated with the incidence of ICH. The hematoma expansion to the subarachnoid space in DM rats infused with autologous blood was 10-fold greater than that observed in NDM rats (Fig. 1a, b). The contralateral hemisphere that received an injection with phosphate buffered saline (PBS) exhibited less hematoma expansion; however there was a trend for increase in DM rats compared with NDM controls. Infusion of autologous blood labeled with Evans blue dye showed that the exogenous blood remained localized to the site of injection whereas the hematoma observed within 30 min on the surface of brain in DM rats was not labeled, indicating that the appearance of blood in the subarachnoid space was rapid and likely derived from vessels ruptured during needle insertion (Supplementary Fig. 1 online). The increased hematoma expansion seen in the STZ-induced DM rats was confirmed in diabetic Akita mice (C57BL/6J-*Ins2*^{Akita}) subjected to autologous blood injection as compared with NDM littermate controls (Fig. 1c).

Our previous report has implicated a role of plasma kallikrein (PK) in blood brain barrier dysfunction following experimental ICH21. PK is activated by coagulation factor XII via the contact activation system and plays a central role in the intrinsic coagulation cascade, innate inflammation, vascular function, and fibrinolysis22. Based on these findings, we investigated the potential role of PK in hematoma expansion in DM animals. Systemic administration of a small molecule PK inhibitor, ASP-44023, reduced hematoma expansion in DM rats (Fig. 1d). The contralateral hemisphere that received a sham injection with PBS also showed a trend for decreased hematoma expansion in ASP-440-treated rats compared with vehicle-treated rats. In addition, co-injection of a neutralized PK-specific antibody with blood in DM rats significantly attenuated hematoma expansion compared with contralateral hemisphere that was subjected to co-injection of blood with a normal IgG control (Fig. 1e).

To further characterize the role of PK in hematoma expansion, we utilized PK-deficient mice that were generated via the disruption of the *Klkb1* gene. The generation and

characterization of *Klkb1*$^{-/-}$ mice are described in supplementary information (Supplementary Fig. 2 online). We show that hematoma volume was significantly lower in STZ-induced diabetic *Klkb1*$^{-/-}$ mice subjected to autologous blood injection compared with diabetic wild-type (WT) mice (Fig. 1f, g). *Klkb1*$^{-/-}$ mice displayed prolonged activated partial thromboplastin time (aPTT) (Fig. 1h), which is similar to the effects of PK-deficiency in human24–25. We also found that both aPTT and tail bleeding time are shorter in DM rats compared with NDM controls. Treatment of DM rats with ASP-440 increased aPTT and tail bleeding time, while reducing hematoma expansion induced by autologous blood (Supplementary Fig. 3a, b online). Shortened aPTT also occurs in patients with impaired fasting plasma glucose and diabetes26. These findings reveal an inverse correlation of aPTT and hematoma expansion during experimental ICH in hyperglycemia.

Hematoma expansion to the subarachnoid space induced by intracerebral injection of purified PK in DM rats was 9-fold greater than that observed in NDM controls (Fig. 2a, b). Moreover, hemorrhage volume assessed by erythrocyte components, hemoglobin (Fig. 2c) and carbonic anhydrase-1 (Fig. 2d), in a 5 mm anterior section of the hemisphere encompassing the injection site in DM rats subjected to PK was 2–4 fold greater than that in NDM rats. The time course showed that PK-induced hematoma expansion in DM rats was rapid, occurring within 30 min (Fig. 2e), which is comparable to the response to autologous blood injection (Supplementary Fig. 1 online). To examine whether hyperglycemia was required for PK-induced hematoma expansion, rats maintained with STZ-induced diabetes for 4-weeks were injected with insulin to lower blood glucose from 428 ± 35 to 158 ± 19 mg/dL (Supplementary Fig. 4 online) immediately prior to intracerebral injection of PK and the subsequent analysis of hematoma expansion was performed at 2 h post-infusion. We found that normalization of blood glucose in DM rats prevented cerebral hematoma expansion induced by PK (Fig. 2f). The role of hyperglycemia on cerebral hematoma expansion was also examined in NDM rats subjected to an intraperitoneal injection of 3 g/kg glucose, which resulted in a blood glucose increase from 91.4 ± 6.7 mg/dL at baseline to 443 ± 15 mg/dL at 30 min after injection (Fig. 2g). Hematoma expansion following intracerebral PK injection was increased in hyperglycemic rats compared with control rats (Fig. 2h). These observations indicate that hyperglycemia, rather than diabetes *per se*, is the critical factor in facilitating hematoma expansion.

Acute hypertension, a local coagulation deficit, or both may be associated with hematoma expansion27. Although both heart rate and blood pressure were increased following intracerebral PK injection, the differences prior to and after injection were similar between NDM and DM groups (Supplementary Fig. 5 online), suggesting that elevated blood pressure does not explain the increased hematoma expansion in DM rats. PK activates various substrates, such as factor XII, high molecular weight kininogen (HK), prourokinase, and plasminogen28. One of the most widely characterized functions of PK is the proteolytic cleavage of HK leading to the production of bradykinin (BK), which causes vascular dilation and permeability via both bradykinin-1 and -2 receptors (B1R and B2R). We show that systemic or local administration of B1R and B2R antagonists [des-Arg^{10}]-Hoe140 and Hoe140, respectively, did not reduce blood-induced hematoma expansion in DM rats, although a trend for a small decrease was observed in the presence of Hoe 140 (Fig. 1d and

Supplementary Fig. 6a online). Intracerebral injection of BK caused a trend for increasing hematoma expansion in both normoglycemic and hyperglycemic rats, however hyperglycemia did not increase the effect of BK (Supplementary Fig. 6b online). These results suggest that BK does not mediate the increase in blood-induced hematoma expansion during hyperglycemia. The potential effect of plasmin activation by PK on hematoma expansion in DM rats was also examined. PK cleaves plasminogen at a limited rate and this cleavage was not affected by glucose (Supplementary Fig. 7a, b online). Continuous assays of clot formation and lysis showed that PK did not inhibit thrombin-induced clot formation and clot lysis (Supplementary Fig. 7c, d online). *In vivo*, neither tPA nor plasmin induced hematoma expansion in DM rats as observed with PK infusion (Supplementary Fig. 7e online). To further evaluate the role of PK catalytic activity in hematoma expansion, PK was deactivated by 4-(2-Aminoethyl) benzenesulfonyl fluoride hydrochloride (Supplementary Fig. 8a online). Intracerebral injection of deactivated PK also induced hematoma expansion in DM rats, as seen in rats receiving PK injection (Fig. 2i). Moreover, the enzyme activity of PK toward its substrate was not increased by high concentrations of glucose (Supplementary Fig. 8b online). These results suggest that the effect of PK on hematoma expansion during hyperglycemia does not involve the previously characterized effects of PK mediated by the BK or plasminogen systems.

Platelet aggregation is a key mechanism for normal hemostasis limiting blood loss following hemorrhage29. Prior antiplatelet therapy is associated with increased hematoma volume and hematoma expansion13,30. While platelets from humans and rodents display a number of differences, the analysis of platelets from rodent models has provided insight into the human processes of hemostasis and platelet aggregation31. We demonstrated that PK inhibited collagen-stimulated platelet aggregation in a dose-dependent manner from 150 to 500 nM (Fig. 3a), whereas PK had no effect on ADP- or thrombin-induced platelet aggregation (Fig. 3b). Glucose (5–25 mM) enhanced the inhibitory effect of PK on collagen-stimulated platelet aggregation in a dose-dependent manner (Fig. 3c), although glucose did not alter platelet aggregation in the absence of PK (data not shown). PK exerted a similar effect on collagen-stimulated aggregation of washed platelets from both NDM and DM rats (Supplementary Fig. 8c online), suggesting that platelets from both sources were similarly affected by PK. Deactivated PK showed similar inhibitory effect on collagen-stimulated platelet aggregation as observed with PK, whereas prekallikrein was not inhibitory (Fig. 3d). ASP-440 did not inhibit the effect of PK on collagen-induced platelet aggregation (Supplementary Fig. 8d online) although the dose of ASP-440 used was sufficient to completely inhibit the catalytic activity of PK (Supplementary Fig. 8e online). These findings suggest that the activation of prekallikrein to PK is required to inhibit collagen-induced platelet activation; however once PK is formed, its proteolytic activity is no longer required. From these data we conclude that PK generation at the site of cerebrovascular hemorrhage is derived from prekallikrein in the blood via the activation of contact system, and the proteolytic activity of PK is required for this process. Since ASP-440 is a selective inhibitor of PK activity23 and prolongs aPTT (Supplementary Fig. 3a online), we conclude that ASP-440 reduces hematoma expansion by suppressing the formation of PK from prekallikrein, possibly mediated by inhibition of the contact activation system.

Platelets interact with subendothelial collagen in damaged blood vessels via a number of molecules including glycoprotein Ib, glycoprotein VI (GPVI), and α2β1 integrin. GPVI plays a critical role in initiating downstream platelet activation29,32–33. The clinical profile of humans with GPVI defects is usually described as having a mild bleeding disorder and their platelets show severely impaired responses to collagen34. To determine the role of GPVI in hematoma expansion following cerebral vascular injury, we examined the effect of intracerebral injection of GPVI blocking monoclonal antibody, JAQ1, and the effect of GPVI deficiency induced by FcR γ-chain gene disruption35 on hematoma expansion in mice. We demonstrate that both local inhibition of GPVI by injection of JAQ1 in the brain and systemic GPVI deficiency resulted in increased hematoma volume and area compared with control IgG injection or WT mice, respectively (Fig. 3e, f). Collagen related peptide (CRP), which mimics collagen triple helix, activates platelets by binding specifically to GPVI32; whereas snake venom convulxin activates platelet GPVI via a mechanism independent of its collagen binding site36. We show that intracerebral infusion of convulxin (35 ng) with PK in DM rats prevented hematoma expansion (Fig. 3g), indicating that increased local activation of GPVI can interfere with the hemorrhagic effect of PK. PK inhibited CRP (100 ng/ml) but not convulxin (0.25 nM)-induced platelet aggregation, however, the inhibitory effect of PK on CRP-induced platelet aggregation was not affected by glucose (Fig. 3h), suggesting that collagen is required for the response to elevated glucose concentrations. While these findings implicate the role of GPVI in PK-induced hematoma expansion, it is possible that PK may also interfere with other mechanisms of platelet-collagen interaction. We demonstrate a dose-dependent binding of PK (0.3–1 μM) to collagen by surface plasmon resonance spectroscopy (Fig. 4a). This specific binding was increased in the presence of 25 mM glucose (Fig. 4b). *Ex vivo* studies confirmed this finding by showing that the binding of PK to rat aorta from which the endothelium has been scraped to expose the underlying basement membrane was increased with glucose in a concentration-dependent manner (Fig. 4c). Our results suggest that high concentration of glucose increases PK binding to collagen, thereby enhancing PK inhibition of collagen-induced platelet aggregation. Although the mechanism by which glucose increases the binding of collagen to PK is not elucidated in this study, previous reports have suggested that a short period of hyperglycemia can alter collagen conformation that may facilitate protein binding37.

The effect of acute hyperglycemia in NDM rats on hematoma expansion (Fig. 2h) suggested that hyperosmolarity may contribute to the effects of high glucose in our ICH model. We show that both hyperosmolar mannitol (25 mM) and hyperosmolar salt (12.5 mM) (osmolarity: 328 mOsm/L) exerted a similar effect as higher concentration of glucose in augmenting the inhibitory effect of PK on collagen-induced platelet aggregation compared with normal osmolar buffer (303 mOsm/L), which is comparable with normal osmolality of serum (280–303 mOsm/kg) (Fig. 4d). NDM rats treated intravenously with 20% mannitol generated similar hematoma expansion at 2 h after PK or blood injection as observed in DM rats (Fig. 4e, f). These results suggest that the increase in hematoma expansion associated with hyperglycemia is mediated by its accompanying increase in osmolality, which is consistent with the report that raised plasma osmolality on admission is associated with stroke mortality38. Mannitol has been used to reduce elevated intracerebral pressure and

edema in patients with stroke, but its effect on hematoma expansion during ICH has not been reported. Our findings suggest that providing mannitol during active ICH may interfere with collagen-stimulated platelet aggregation.

We demonstrate that hyperglycemia increased hematoma expansion during the experimental ICH and the exacerbation of hematoma expansion was mediated by PK. We have identified a novel osmotic-sensitive mechanism for PK inhibition of collagen-induced platelet aggregation, which could contribute to impaired hemostasis. Our findings suggest that PK represents a target for interfering with hematoma expansion in the setting of hyperglycemia. The major limitations of the experimental ICH model used in this report are that the initiating event causing cerebrovascular injury does not emulate the etiology of the majority of spontaneous ICH in humans39 and responses in healthy rodent models may not fully mimic vasculopathies and hemostatic events in patients with ICH. Given the challenges inherent in modeling hemorrhage in animal models, additional studies will be needed to determine the role of PK in ICH during hyperglycemia in the clinical setting.

METHODS

Intracerebral hemorrhage model

We induced diabetes in Sprague-Dawley rats by intraperitoneal injection of 55 mg/kg of STZ in 10 mM citrate buffer (pH 4.5) after overnight fasting, or in mice by intraperitoneal injection of 100 mg/kg of STZ in citrate buffer for 2 days. We confirmed diabetes by measuring blood glucose (> 250 mg/dL) 24 h after STZ injection. Blood glucose at the time of surgery was 442 ± 12 and 109 ± 3 mg/dL for DM and NDM rats, respectively. Initial body weight of rats was 250 g and average body weight after 4 weeks was 403 ± 10 g for NDM rats and 294 ± 5 g for DM rats, respectively. C57BL/6J-*Ins2*^{Akita} mice were purchased from the Jackson Laboratory. FcR γ-chain–deficiency (*Fcer1g*$^{-/-}$) mice were purchased from Taconic. We performed all experiments in accordance with the guidelines of the National Institutes of Health Guide for the Care and Use of Laboratory Animals and with approval from the Animal Care and Use Committee of the Joslin Diabetes Center.

We anaesthetized the rats with pentobarbital (50 mg/kg, ip), surgically exposed the surface of the skull and slowly injected 50 μl PBS, 50 μl autologous whole blood (from tail vein), 15 μg purified human PK (Enzyme Research Laboratories), 30 μg deactivated PK or 5 μM bradykinin (Calbiochem) in 50 μl PBS into the brain at 1 mm anterior, 4 mm lateral and 6 mm in depth to the bregma using a 30 gauge needle. For mice, we slowly injected 10 μl saline or autologous whole blood into the brain at 1 mm anterior, 2 mm lateral and 3.5 mm in depth to the bregma using a 30 gauge needle. We removed the infusion needle 10 min after injection and sealed the burr hole with bone wax. We delivered Hoe140 (1 μg/kg/hr), [des-Arg^{10}]-Hoe140 (1 μg/kg/hr) (Sigma), 1-Benzyl-1H-pyrazole-4-carboxylic acid 4-carbamimidoyl-benzylamide (ASP-440) (14 μg/kg/hr) or its vehicle (10 % polyethylene glycol in PBS) by subcutaneous osmotic pump (ALZET) into rats 1 day prior to injection. For the mixture of Hoe 140 and [des-Arg^{10}]-Hoe140 injection, 2 μM of each compound was mixed with 50 μl blood before injection. For PK-specifc antibody injection, antibody to PK (Abcam, final concentration: 0.06 mg/ml) or mouse IgG (final concentration: 0.06 mg/ml) was mixed with 50 μl blood prior to injection. For convulxin injection, 35 ng convulxin

(Alexis Biochemicals) was mixed with 15 μg PK in 50 μl PBS prior to injection. For GPVI-specific antibody injection, we injected 10 μg JAQ1 antibody (Amfret Analytics) or rat IgG in 30 μPBS into mice brains. For mannitol infusion experiment, we injected a bolus of 15 ml/kg of 20% mannitol intravenously (calculated plasma osmolality: 320 mOsm/kg) to the rats followed by cerebral injection of autologous blood or PK. We continuously infused the rats intravenously with 20% mannitol at a rate of 15 ml/kg/h for 2 h to maintain constant osmolality. We examined cerebral hematoma area or volume at 30 min, 2 h, or 48 h after injection. We perfused the animals with saline through the left ventricle, harvested the brains, and determined hematoma areas with Quantity One software (BioRad).

Platelet aggregation

We collected blood from the vena cava of the rats and anti-coagulated with acid-citrate-dextrose buffer (9:1, v/v). Platelet-rich plasma (PRP) was obtained by centrifugation of the blood at 250 g for 15 min. We then centrifuged the PRP at 500 g for 10 min to obtain platelet pellets, and washed the pallets 3 times with a modified Tyrode's buffer without Ca^{2+} (134 mM NaCl, 3 mM KCl, 0.3 mM NaH_2PO4, 2 mM $MgCl_2$, 5 mM HEPES, 5 mM glucose, 12 mM $NaHCO_3$, 1 mM EGTA, and 3.5 mg/mL BSA). We resuspended the final pellets in Tyrode's buffer with 1 mM $CaCl_2$ but no EGTA and adjusted to a final platelet concentration at $2x10^8$ cells/ml. We monitored platelet aggregation using a Chrono-Log 680 Aggregation System (Chrono-Log) with stirring at 37°C. We activated platelets with equine type I collagen (2 μg/ml, Chrono-Log), thrombin (0.25 U/ml, Sigma), or ADP (20 μM, Sigma), and recorded the change of transmission. We also monitored platelet aggregation using a 96-well microplate reader (PerkinElmer)40. Briefly, the aggregation process was carried out in 100 μl volume in a 96 well flat-bottom microplate. Platelets were activated with type I collagen (2 μg), collagen related peptide (CRP, 10 ng, University of Cambridge, UK), or convulxin (0.25 nM), and the readings were taken every 30 seconds over a 20-minute period at 405 nm wavelength. The collected data were recorded and converted to aggregation curves. The results obtained using the microplate reader were consistent with those from platelet aggregometer.

Surface plasmon resonance spectroscopy

We measured the interaction between PK and collagen with a BIAcore 3000 system (BIAcore AB) using HES buffer (10 mM HEPES, 150 mM NaCl, 2 mM EDTA, pH 7.4) at 25°C. Rat tail type I collagen in 10 mM sodium acetate buffer (pH 5.0) was covalently coupled to a CM5 chip using an Amine Coupling Kit (BIAcore AB) according to the manufacturer's instructions. A control surface underwent the same activation and deactivation procedures in the absence of collagen. Regeneration of the collagen surface was achieved by running 10 μl of 10 mM glycine (pH 2.0) through the flow cell at 10 μl/min. PK solutions at several concentrations were perfused over the immobilized collagen at a flow rate of 10 μl/min for 3 min, and the resonance changes were recorded. The sensorgram of the immobilized-collagen surface was subtracted from that of the control surface, and the data thus obtained were analyzed by BIAevaluation software (BIAcore AB).

Incubation of rat aortic segments with PK

We isolated rat aorta and placed it in 4°C PBS. We rinsed the aorta free of blood, trimmed surrounding connective tissue and the intercostal vessels, opened longitudinally, and gently scraped the inner surface with a sterile razor blade to remove the endothelium. We washed the vessel 3 times with ice cold PBS and divided it into approximately 4 mm^2 pieces. Care was given to assure that the exposed aorta was covered by PBS during this procedure. We incubated aorta pieces with buffer containing 300 nM PK and glucose (0–50 mM) for 30 min at 25°C. We then washed the segments, and measured the activity of surface-bound PK.

Statistical analysis

All results are presented as means ± s.e.m. Statistical analysis was performed by one-way analysis of variance (ANOVA) followed by Bonferroni's multiple comparisons test or Students' *t*-test as appropriate. Statistically significant differences between groups were defined as $P < 0.05$ and are indicated in the legends of the figures.

The methods for generation and characterization of *Klkb1*$^{-/-}$ mice, systemic hemostasis measurement, hemoglobin analysis, Western blotting, cardiac output measurement, plasminogen activation, continuous assays of clot formation and lysis, and PK activity assay are provided in the Supplementary Methods online.

Supplementary Material

Refer to Web version on PubMed Central for supplementary material.

ACKNOWLEDGMENTS

This work was supported in part by the US National Institutes of Health (grants EY19029, DK36836, HL090132, HL87203, HL07917) and the American Heart Association (0855905D, 0840043N).

Reference

1. Feigin VL, Lawes CM, Bennett DA, Anderson CS. Stroke epidemiology: a review of population-based studies of incidence, prevalence, and case-fatality in the late 20th century. Lancet Neurol. 2003; 2:43–53. [PubMed: 12849300]
2. Arboix A, Massons J, Garcia-Eroles L, Oliveres M, Targa C. Diabetes is an independent risk factor for in-hospital mortality from acute spontaneous intracerebral hemorrhage. Diabetes Care. 2000; 23:1527–1532. [PubMed: 11023147]
3. Kimura K, et al. Hyperglycemia independently increases the risk of early death in acute spontaneous intracerebral hemorrhage. J Neurol Sci. 2007; 255:90–94. [PubMed: 17350046]
4. Godoy DA, Pinero GR, Svampa S, Papa F, Di Napoli M. Hyperglycemia and short-term outcome in patients with spontaneous intracerebral hemorrhage. Neurocrit Care. 2008; 9:217–229. [PubMed: 18300001]
5. Lee SH, et al. Effects of glucose level on early and long-term mortality after intracerebral haemorrhage: the Acute Brain Bleeding Analysis Study. Diabetologia. 2010; 53:429–434. [PubMed: 20091021]
6. Demchuk AM, et al. Serum glucose level and diabetes predict tissue plasminogen activator-related intracerebral hemorrhage in acute ischemic stroke. Stroke. 1999; 30:34–39. [PubMed: 9880385]
7. Poppe AY, et al. Admission hyperglycemia predicts a worse outcome in stroke patients treated with intravenous thrombolysis. Diabetes Care. 2009; 32:617–622. [PubMed: 19131465]

8. Broderick JP, Brott TG, Duldner JE, Tomsick T, Huster G. Volume of intracerebral hemorrhage. A powerful and easy-to-use predictor of 30-day mortality. Stroke. 1993; 24:987–993. [PubMed: 8322400]
9. Davis SM, et al. Hematoma growth is a determinant of mortality and poor outcome after intracerebral hemorrhage. Neurology. 2006; 66:1175–1181. [PubMed: 16636233]
10. Kazui S, Minematsu K, Yamamoto H, Sawada T, Yamaguchi T. Predisposing factors to enlargement of spontaneous intracerebral hematoma. Stroke. 1997; 28:2370–2375. [PubMed: 9412616]
11. Passero S, Ciacci G, Ulivelli M. The influence of diabetes and hyperglycemia on clinical course after intracerebral hemorrhage. Neurology. 2003; 61:1351–1356. [PubMed: 14638954]
12. Fogelholm R, Murros K, Rissanen A, Avikainen S. Admission blood glucose and short term survival in primary intracerebral haemorrhage: a population based study. J Neurol Neurosurg Psychiatry. 2005; 76:349–353. [PubMed: 15716524]
13. Broderick JP, et al. Determinants of intracerebral hemorrhage growth: an exploratory analysis. Stroke. 2007; 38:1072–1075. [PubMed: 17290026]
14. Stead LG, et al. Emergency Department hyperglycemia as a predictor of early mortality and worse functional outcome after intracerebral hemorrhage. Neurocrit Care. 2010; 13:67–74. [PubMed: 20390379]
15. Scott JF, et al. Prevalence of admission hyperglycaemia across clinical subtypes of acute stroke. Lancet. 1999; 353:376–377. [PubMed: 9950447]
16. Gray CS, et al. Glucose-potassium-insulin infusions in the management of post-stroke hyperglycaemia: the UK Glucose Insulin in Stroke Trial (GIST-UK). Lancet Neurol. 2007; 6:394–406. [PubMed: 17434093]
17. Bruno A, et al. Treatment of hyperglycemia in ischemic stroke (THIS): a randomized pilot trial. Stroke. 2008; 39:384–389. [PubMed: 18096840]
18. McCormick MT, Muir KW, Gray CS, Walters MR. Management of hyperglycemia in acute stroke: how, when, and for whom? Stroke. 2008; 39:2177–2185. [PubMed: 18436889]
19. Godoy DA, Pinero GR, Svampa S, Papa F, Di Napoli M. Early hyperglycemia and intravenous insulin-the rationale and management of hyperglycemia for spontaneous intracerebral hemorrhage patients: is time for change? Neurocrit Care. 2009; 10:150–153. [PubMed: 18463989]
20. Broderick J, et al. Guidelines for the management of spontaneous intracerebral hemorrhage in adults: 2007 update: a guideline from the American Heart Association/American Stroke Association Stroke Council, High Blood Pressure Research Council, and the Quality of Care and Outcomes in Research Interdisciplinary Working Group. Stroke. 2007; 38:2001–2023. [PubMed: 17478736]
21. Gao BB, et al. Extracellular carbonic anhydrase mediates hemorrhagic retinal and cerebral vascular permeability through prekallikrein activation. Nat Med. 2007; 13:181–188. [PubMed: 17259996]
22. Schmaier AH, McCrae KR. The plasma kallikrein-kinin system: its evolution from contact activation. J Thromb Haemost. 2007; 5:2323–2329. [PubMed: 17883591]
23. Phipps JA, et al. Plasma kallikrein mediates angiotensin II type 1 receptor-stimulated retinal vascular permeability. Hypertension. 2009; 53:175–181. [PubMed: 19124682]
24. Acar K, Yagci M, Sucak GT, Haznedar R. Isolated prolonged activated partial thromboplastin time in an asymptomatic patient: Fletcher factor deficiency. Thromb Res. 2006; 118:765–766. [PubMed: 16414101]
25. Asmis LM, Sulzer I, Furlan M, Lammle B. Prekallikrein deficiency: the characteristic normalization of the severely prolonged aPTT following increased preincubation time is due to autoactivation of factor XII. Thromb Res. 2002; 105:463–470. [PubMed: 12091043]
26. Lippi G, et al. Epidemiological association between fasting plasma glucose and shortened APTT. Clin Biochem. 2009; 42:118–120. [PubMed: 19014926]
27. Qureshi AI, et al. Spontaneous intracerebral hemorrhage. N Engl J Med. 2001; 344:1450–1460. [PubMed: 11346811]
28. Gallimore MJ, Fareid E, Stormorken H. The purification of a human plasma kallikrein with weak plasminogen activator activity. Thromb Res. 1978; 12:409–420. [PubMed: 418517]

29. Ruggeri ZM, Mendolicchio GL. Adhesion mechanisms in platelet function. Circ Res. 2007; 100:1673–1685. [PubMed: 17585075]
30. Toyoda K, et al. Antiplatelet therapy contributes to acute deterioration of intracerebral hemorrhage. Neurology. 2005; 65:1000–1004. [PubMed: 16217049]
31. Nieswandt B, Aktas B, Moers A, Sachs UJ. Platelets in atherothrombosis: lessons from mouse models. J Thromb Haemost. 2005; 3:1725–1736. [PubMed: 16102039]
32. Kehrel B, et al. Glycoprotein VI is a major collagen receptor for platelet activation: it recognizes the platelet-activating quaternary structure of collagen, whereas CD36, glycoprotein IIb/IIIa, and von Willebrand factor do not. Blood. 1998; 91:491–499. [PubMed: 9427702]
33. Nieswandt B, Watson SP. Platelet-collagen interaction: is GPVI the central receptor? Blood. 2003; 102:449–461. [PubMed: 12649139]
34. Arthur JF, Dunkley S, Andrews RK. Platelet glycoprotein VI-related clinical defects. Br J Haematol. 2007; 139:363–372. [PubMed: 17910626]
35. Nieswandt B, et al. Expression and function of the mouse collagen receptor glycoprotein VI is strictly dependent on its association with the FcRgamma chain. J Biol Chem. 2000; 275:23998–24002. [PubMed: 10825177]
36. Miura Y, Takahashi T, Jung SM, Moroi M. Analysis of the interaction of platelet collagen receptor glycoprotein VI (GPVI) with collagen. A dimeric form of GPVI, but not the monomeric form, shows affinity to fibrous collagen. J Biol Chem. 2002; 277:46197–46204. [PubMed: 12356768]
37. Stultz CM, Edelman ER. A structural model that explains the effects of hyperglycemia on collagenolysis. Biophys J. 2003; 85:2198–2204. [PubMed: 14507685]
38. Bhalla A, et al. Influence of raised plasma osmolality on clinical outcome after acute stroke. Stroke. 2000; 31:2043–2048. [PubMed: 10978027]
39. James ML, Warner DS, Laskowitz DT. Preclinical models of intracerebral hemorrhage: a translational perspective. Neurocrit Care. 2008; 9:139–152. [PubMed: 18058257]
40. Walkowiak B, Kesy A, Michalec L. Microplate reader--a convenient tool in studies of blood coagulation. Thromb Res. 1997; 87:95–103. [PubMed: 9253804]

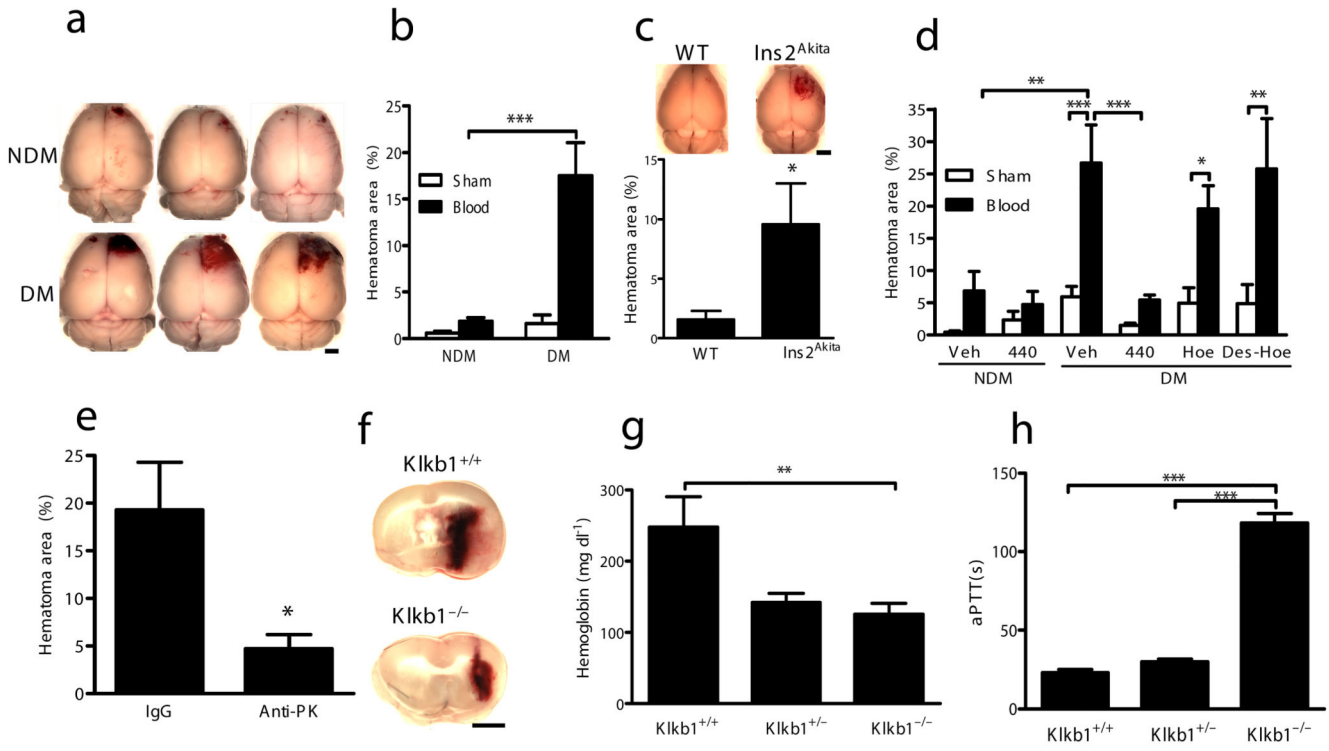

Figure 1. Effect of kallikrein-kinin inhibition on hematoma expansion in diabetic animals

(**a**) Representative images of the dorsal surface and (**b**) the ratio of surface hematoma area to hemisphere area of brains at 48 h after intracerebral injection of autologous blood into the right hemisphere or sham injection into the left hemisphere from NDM (n = 15) and DM rats (n = 11). Scale bar, 2 mm. (**c**) Representative images and the ratio of surface hematoma area to hemisphere area of brains from DM Akita mice (*Ins2*^{Akita}, n = 10) and the NDM littermate WT controls (n = 9) following PBS injection into left hemisphere and autologous blood injection into right hemisphere. Scale bar, 2 mm. (**d**) The ratio of surface hematoma area to hemisphere area of brains at 48 h after intracerebral injection of autologous blood to NDM rats systemically treated with vehicle (Veh, n = 4) or ASP-440 (440, n = 6), and to DM rats systemically treated with vehicle (n = 7), ASP-440 (n = 11), Hoe-140 (Hoe, n = 8), or [des-Arg^{10}]-Hoe140 (Des-Hoe, n = 5). (**e**) The ratio of surface hematoma area to hemisphere area of brains at 48 h after intracerebral injection of autologous blood mixed with PK-specific antibody into the right hemisphere or IgG into the left hemisphere of DM rats (n = 6). (**f**) Representative images of the coronal slices of brains at 2 h after intracerebral injection of blood into the right hemisphere or PBS injection into the left hemisphere from diabetic *Klkb1*$^{+/+}$ and *Klkb1*$^{-/-}$, mice. Scale bar, 2 mm. (**g**) Hemoglobin content of hemispheres subjected to autologous blood from *Klkb1*$^{+/+}$ (n = 16), *Klkb1*$^{+/-}$ (n = 10) and *Klkb1*$^{-/-}$ (n = 23) mice. (**h**) aPTT from *Klkb1*$^{+/+}$, *Klkb1*$^{+/-}$, and *Klkb1*$^{-/-}$ mice (n = 6). * P < 0.05; ** P < 0.01; *** P < 0.001.

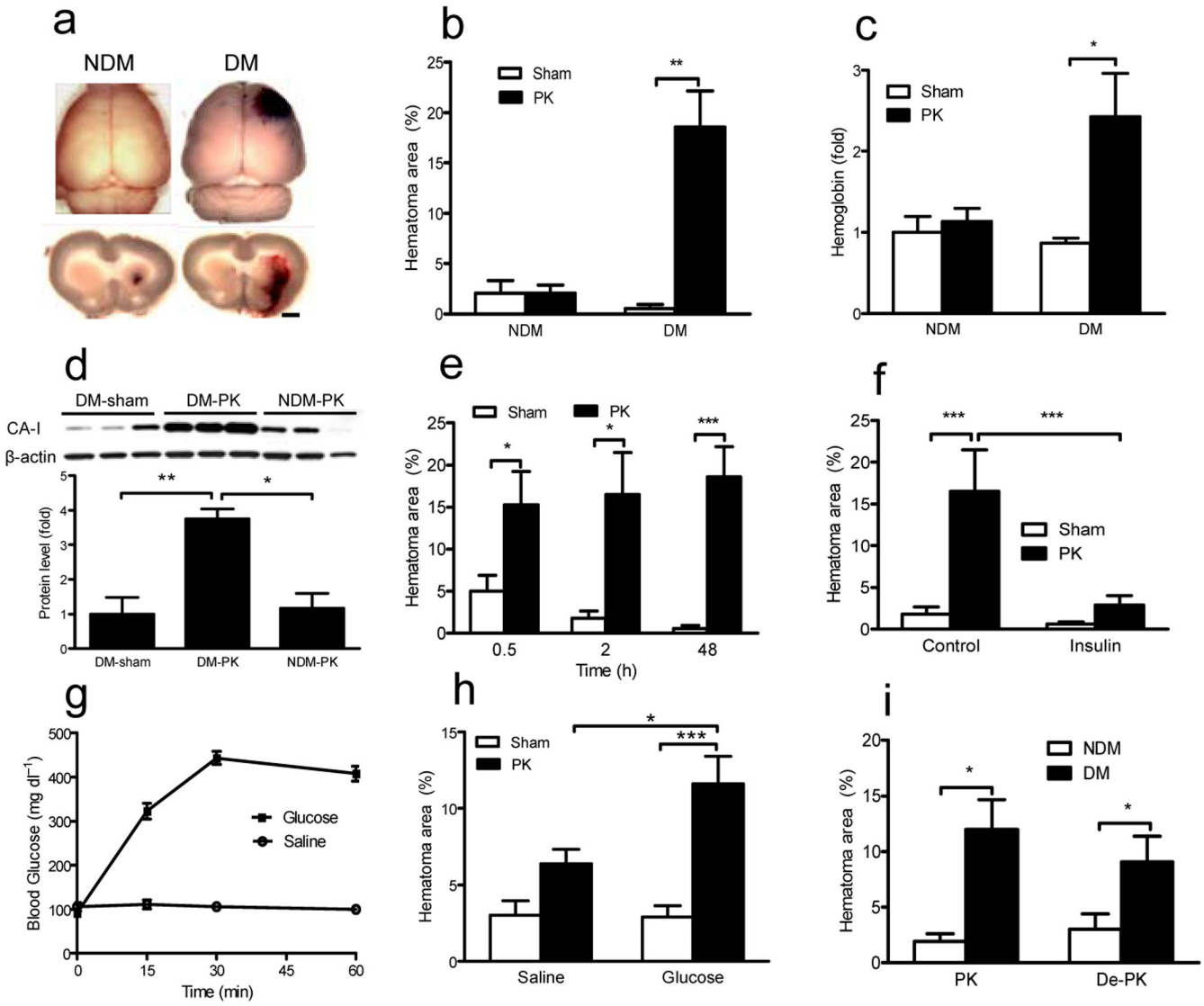

Figure 2. Effect of intracerebral injection of PK on hematoma expansion in diabetic rats

(**a**) Representative images of the dorsal surface and coronal slice and (**b**) the ratio of surface hematoma area to hemisphere area of brains at 48 h after intracerebral injection of PK into the right hemisphere or PBS injection into the left hemisphere from NDM (*n* = 5) and DM rats (*n* = 7). Scale bar, 2 mm. (**c**) Hemoglobin and (**d**) carbonic anhydrase 1 (CA-1) levels in the 5 mm anterior transverse section hemispheres encompassing the injection site. *n* = 3–7 rats. (**e**) Time course of hematoma expansion after intracerebral injection of PK into right hemisphere or PBS injection into left hemisphere of DM rats. *n* = 7–8 rats. (**f**) Effect of insulin treatment on hematoma expansion following intracerebral PK injection in DM rats. *n* = 8–12 rats. (**g**) Time course of blood glucose level after intraperitoneal injection of saline (*n* = 11) or glucose (*n* = 15) in rats. (**h**) The ratio of hematoma area to hemisphere area of brains at 0.5 h following intracerebral PK or PBS injections from saline (*n* = 10) or glucose intraperitoneal injected rats (*n* = 13). (**i**) The ratio of surface hematoma area to hemisphere

area of brains from NDM (n = 8) and DM rats (n = 6) at 0.5 h after intracerebral injection of PK or deactivated PK (De-PK). n = 6–14 rats. * $P < 0.05$; ** $P < 0.01$; *** $P < 0.001$.

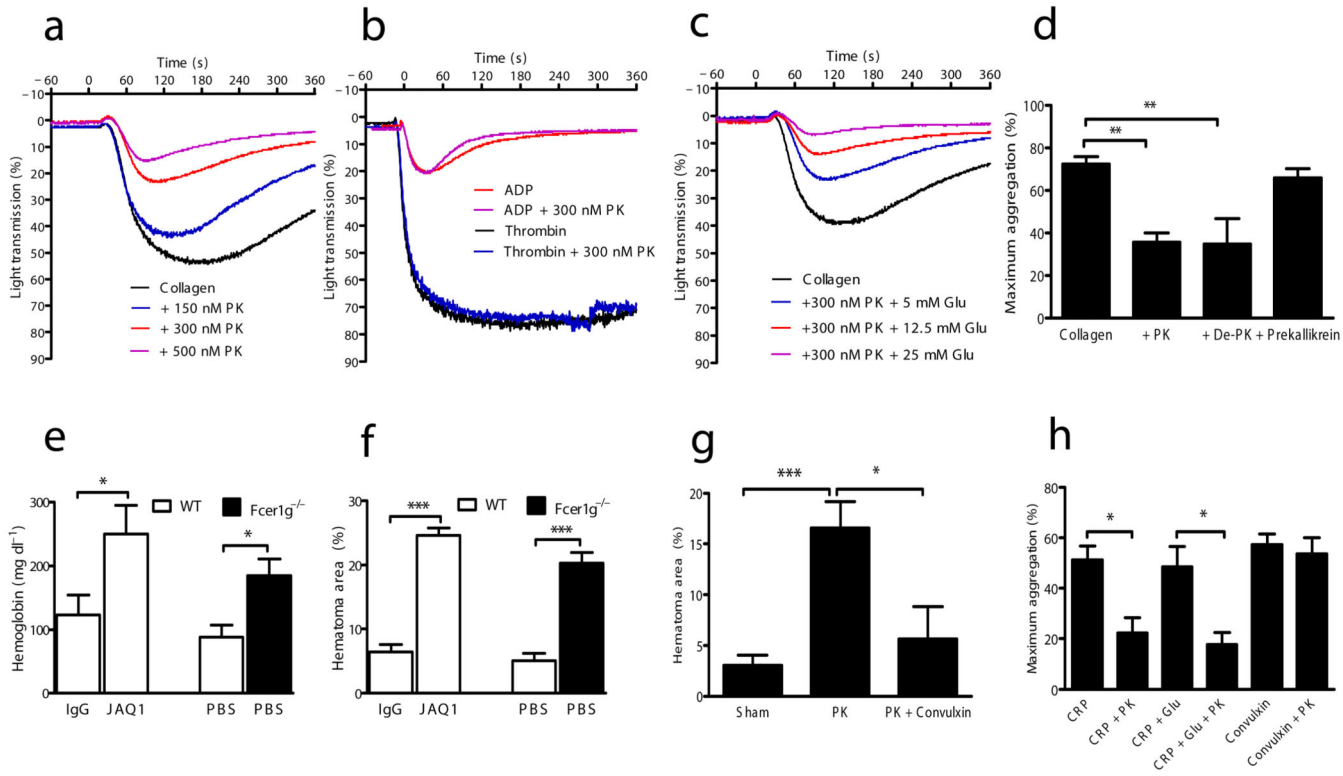

Figure 3. Effect of PK on collagen-stimulated platelet aggregation

(**a**) Effect of PK on collagen-stimulated platelet aggregation. (**b**) Effect of PK on thrombin or ADP-induced platelet aggregation. (**c**) Effect of glucose on PK-induced inhibition of collagen-stimulated platelet aggregation. (**d**) Effects of PK (160 nM), prekallikrein (160 nM) and deactivated PK (De-PK, 160 nM) on collagen-induced platelet aggregation. $n = 4$ independent experiments. (**e**) Hemoglobin content of hemisphere and (**f**) the ratio of hematoma area to hemisphere area of brains from C57BL/6 WT mice subjected to JAQ or rat IgG injection in the contralateral hemisphere ($n = 6$); C57BL/6 WT mice subjected to PBS injection ($n = 10$); and FcR γ-chain-deficiency (*Fcer1g*$^{-/-}$) mice subjected to PBS injection ($n = 5$). (**g**) Effect of convulxin on PK-induced hematoma expansion in DM rats. $n = 6$–19 rats. (h) Effects of PK (160 nM) and glucose (Glu, 25 mM) on CRP or convulxin-induced platelet aggregation. $n = 3$–5 independent experiments. Platelet aggregation was measured by platelet aggregometer for (a–c) and by microplate reader for (d, h). * $P < 0.05$; ** $P < 0.01$; *** $P < 0.001$.

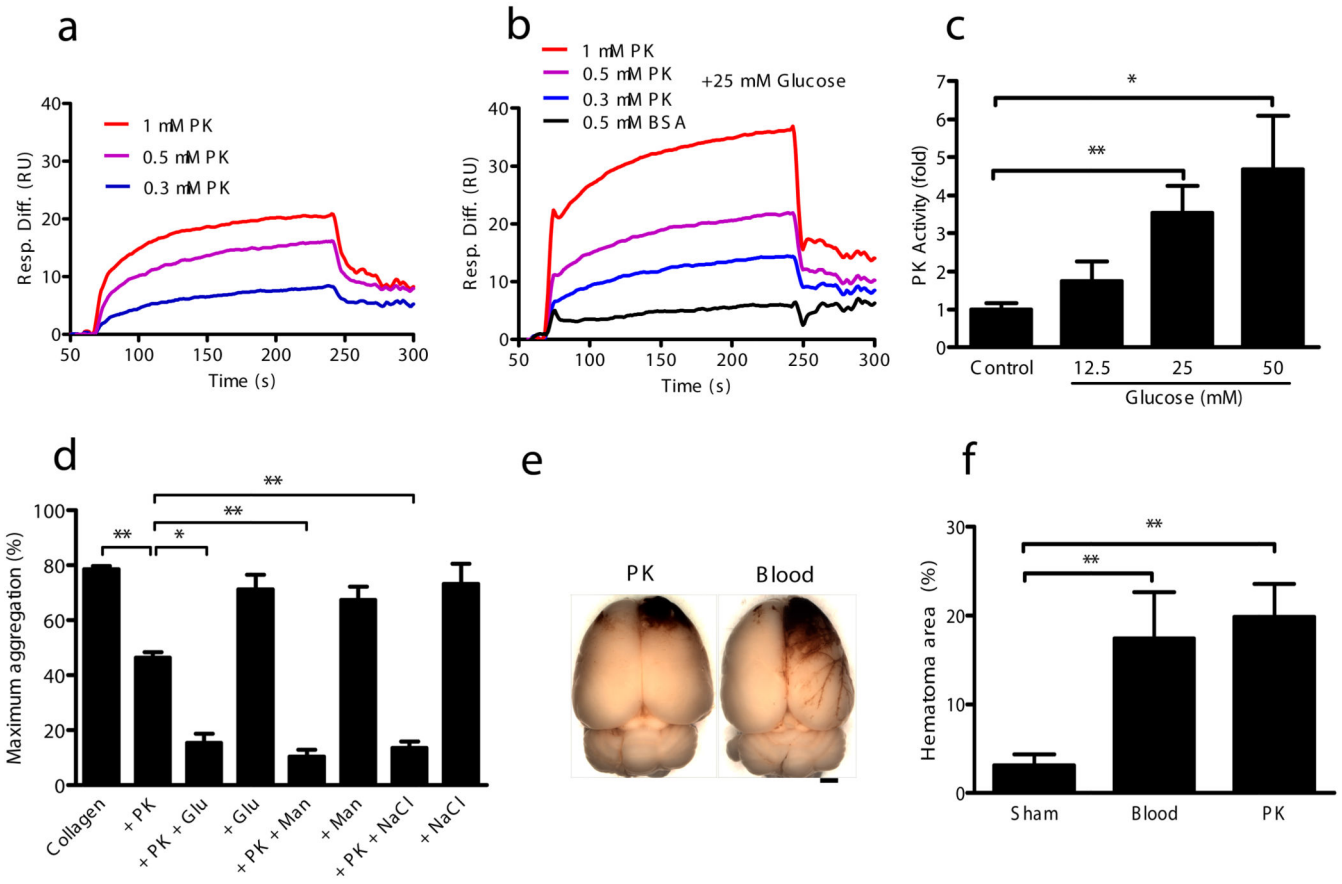

Figure 4. Effect of osmolarity on the binding of PK to collagen, collagen-stimulated platelet aggregation, and hematoma expansion

Sensorgram of the interaction of PK with immobilized collagen type I in the (**a**) absence or (**b**) presence of glucose. (**c**) Effect of glucose on PK binding to aorta tissue. $n = 5$ pieces rat aorta tissue. (**d**) Effects of hyperosmotic mannitol or NaCl on PK-induced inhibition of collagen-stimulated platelet aggregation. $n = 3$ independent experiments. (**e**) Representative images and (**f**) the ratio of surface hematoma area to hemisphere area of the dorsal surface of brains at 2 h after intracerebral injection of PK or autologous blood into the right hemisphere or PBS injection into the left hemisphere of mannitol-treated NDM rats ($n = 6$). * $P < 0.05$; ** $P < 0.01$. Scale bar, 2 mm.